

Spectroscopic study of the planetary nebulae with Wolf-Rayet nuclei in the Magellanic Clouds

M. Peña^{1,*,**}, M.T. Ruiz^{2,*}, and S. Torres-Peimbert^{1,**}

¹ Instituto de Astronomía, Universidad Nacional Autónoma de México, Apdo. Postal 70 264, México D.F. 04510, México

² Departamento de Astronomía, Universidad de Chile, Casilla 36-D, Santiago, Chile

Received 12 August 1996 / Accepted 8 January 1997

Abstract. UV and optical spectrophotometric data of planetary nebulae with WR nuclei in the Magellanic Clouds are presented. Analysis of the nebular characteristics shows that the ionized gas, in all the objects, is extremely C-rich, probably due to contamination with freshly-made C from stellar nucleosynthesis. Very high electron densities are found ($N_e \geq 10^4 \text{ cm}^{-3}$) which are interpreted as an indication of youth. The central stars are C-rich, with spectral types in the range from WC 4–5 to WC 8. The spectral type distribution is totally different from that found for galactic planetary nebulae with WR nuclei. Estimates of the stellar visual magnitudes and temperatures are presented. Stellar temperatures over 60 000 K were derived for all the objects, with some cases exceeding 100 000 K. These high temperatures however do not produce high excitation nebulae.

Key words: Magellanic Clouds – planetary nebulae: general – ISM: abundances – stars: Wolf-Rayet – stars: fundamental parameters

1. Introduction

The Magellanic Cloud planetary nebulae with central stars showing WR features (MC WR-PNe) represent less than 5% of the known sample of PNe in these galaxies. They are: N 6 and Ln 302 (MG 08) in the SMC and N 110 (SMP 38), N 133 (SMP 58), N 203 (SMP 61), LM 1-64, MA 17, and N 66 (SMP 83) in the LMC. The latter one, which recently developed a bright WR nucleus resembling a Population I WN4.5 star (Peña et al. 1994b, 1995), represents a unique event in the PN population field. This object, however, will not be discussed here. A comparison between N 66 characteristics and those of

the LMC WR-PNe can be found in Peña (1995) and Peña et al. (1996).

Most of the MC WR-PNe have been reported to show medium to low excitation classes and their central stars have been classified as type WC 4, WC 4–5 or later (i.e., Monk et al. 1988 and references therein). N 133 was the first LMC PN detected in radio continuum (Zijlstra et al. 1994); together with N 203 they are two of the only 12 LMC PNe reported in the IRAS Faint Source Catalogue. According to Zijlstra et al. (1994), their IRAS colors are indicative of young nebulae. For N 203, Bianchi et al. (1997) have recently reported a stellar temperature of 60 000 K, a mass loss rate $\dot{M} \leq 7 \times 10^{-7} M_{\odot} \text{ yr}^{-1}$ and a wind velocity $v_{\infty} = 1600 \text{ km s}^{-1}$. MA 17 was discovered in the UK Schmidt Objective-Prism Survey (Morgan 1994). Spectroscopic data were reported by Vassiliadis et al. (1992) and its central star has been studied by Hamann (1996) who classified it as a WC 7 type star. SMC Ln 302 is a very low excitation object (Sanduleak & Phillips 1976) whose nucleus was classified as a WC 8 type star by Monk et al. (1988). LM 1-64 is a high excitation C-rich PN with a hot nucleus of effective temperature about 100 000 K showing relatively faint C emission lines (Peña et al. 1994a).

Due to its well known common distance, this sample provides a unique opportunity to analyze the nebular and central star properties aimed at understanding these low luminosity WR type stars.

Although some general optical studies exist (Barlow 1987; Monk et al. 1988; Meatheringham & Dopita 1991a,b; Dopita & Meatheringham 1991; Vassiliadis et al. 1992), physical conditions and chemical composition of most of the MC WR-PNe are not well known. Therefore we started an extensive study of these objects, including UV and optical spectroscopic observations. The spectral ranges from 1200 to 2000 Å and 3200 to 7500 Å were covered with medium resolution. The observed spectra include both the nebula, and the central star emissions. These data allowed us to determine accurate physical nebular conditions which are discussed in Sect. 4, and to derive some stellar parameters, presented in Sect. 5.

Send offprint requests to: M. Peña

* Visiting astronomer at Cerro Tololo Inter-American Observatory operated by AURA under contract with the NSF.

** Guest observer with the International Ultraviolet Satellite operated by NASA.

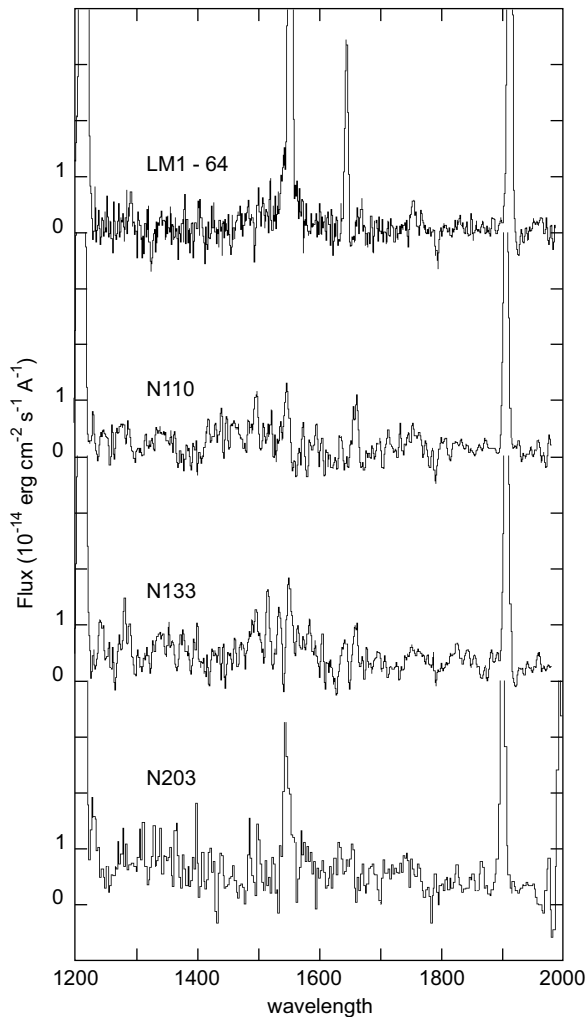


Fig. 1. UV calibrated spectra of objects in this work.

2. Observations

2.1. Ultraviolet data

UV observations were carried out with the IUE satellite in several observing runs. At least one good signal-to-noise low-dispersion large-aperture SWP spectrum was obtained for each LMC object, except for MA 17. The SMC PNe, N 6 and Ln 302, have not been observed at UV wavelengths. In addition to our observations, all the available IUE spectra of the LMC WR-PNe were retrieved from the archives and analyzed. In Table 1 we list the IUE frames employed in this study; the last column indicates the origin of the data. UV spectra were reduced using standard procedures at IUE Regional Data Analysis Facilities at NASA, GSFC. Some SWP calibrated spectra are shown in Fig. 1. All the objects show faint continua and very intense C III] λ 1909 nebular emission lines. In addition, LM 1-64 also shows intense C IV λ 1550 and He II λ 1640 nebular lines. Stellar C IV λ 1550 emission lines are detected in the other objects, specially in N 203 and N 133 where P-Cygni profiles are observed. All

Table 1. Log of IUE observations.

object	SWP	exp. time (min)	observation date	source
N 110	19486	185	March 19, 1983	arch.
"	49113	120	November 5, 1993	own
"	52224	165	September 25, 1994	own
N 133	19481	168	March 18, 1983	arch.
"	52213	170	September 25, 1994	own
N 203	54313	135	April 6, 1995	own
LM 1-64	39567	115	September 2, 1990	own
"	39573	180	September 3, 1990	own

available UV line fluxes were measured and they are presented in Table 2 together with the optical data.

2.2. Optical data

Long-slit spectrophotometric data for N 110, N 133, N 203, LM 1-64 and SMC N 6 were obtained at CTIO, on December 29 and 30, 1994. The 4-m telescope, equipped with a RC spectrograph, a Reticon detector (1200×400 pix) and the grating KPGL#2, was employed. Several spectra with slit widths of $2''$ and $10''$ were acquired for each object. The wavelength range from 3169 to 7468 Å was covered with a resolution of 6-8 Å for the $2''$ slit spectra and of 8-10 Å for the $10''$ slit ones. In all cases the slit was oriented along the parallactic angle to avoid atmospheric refraction effects. Spectrophotometric standard stars from the list by Hamuy et al. (1992) were observed each night for flux calibration. Data reduction was performed at Cerro Calán Observatory, University of Chile, and Instituto de Astronomía, UNAM, using IRAF reduction package.

The calibrated spectrum of LMC N 203 is presented in Fig. 2 as an example. Strong nebular lines are superposed on a faint continuum which is dominated by the nebular emission, as it can be noticed in the Balmer discontinuity. Also broad carbon stellar features are evident at $\lambda\lambda$ 4650 and 5808. In Figs. 3 and 4, expansions of the spectral regions around the stellar features are shown.

All the nebular emission lines were measured in the $2''$ slit and the $10''$ slit spectra. We found that the line intensities, relative to $H\beta$, are very similar in both types of spectra although, for some objects, the absolute fluxes are slightly larger in the $10''$ slit spectra. This indicates that some light was lost in the narrow slit. However, we are certain that the $10''$ slit included the entire object and, therefore, these fluxes can be directly compared with the UV ones. The measured UV and optical intensities, relative to $H\beta$, are presented in Table 2. Line flux uncertainties are smaller than 5% for the strong lines ($F_\lambda/F(H\beta) \geq 0.2$), and about 10% for the faint ones. Values marked with a colon have larger uncertainties. The $H\beta$ absolute fluxes presented in Table 2 were measured in the wide slit spectra and their uncertainties are smaller than 0.08 dex, for all the studied nebulae.

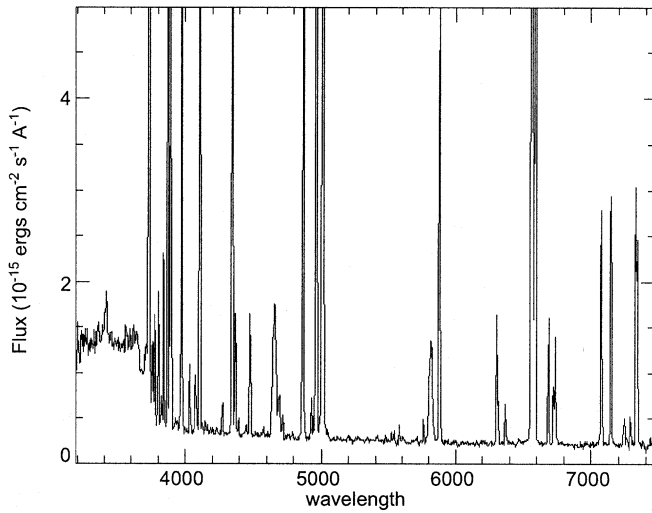


Fig. 2. Calibrated optical spectrum of LMC N 203. The continuum is very faint and dominated by nebular emission.

In Table 2 we have included spectroscopic data for LMC MA 17 and SMC Ln 302 given by Vassiliadis et al. (1992) and Barlow (1987). These data will be used in Sect. 3 to perform plasma diagnosis of these objects.

3. Physical conditions of the nebulae

The observed emission fluxes were corrected for reddening according to the expression:

$$\log I(\lambda) / I(H\beta) = \log F(\lambda) / F(H\beta) + c(H\beta) \times f_{\lambda} \quad (1)$$

where $I(\lambda)$ and $F(\lambda)$ are the dereddened and observed fluxes respectively, and f_{λ} is the reddening law. For the visual region, we employed f_{λ} as given by Whitford (1958) and for the UV region, the LMC reddening law given by Nandy et al. (1981) was used. $C(H\beta)$, the logarithmic reddening correction at $H\beta$, was derived for each object from the Balmer decrement, by considering case B recombination theory (Hummer & Storey 1987). The values obtained for $c(H\beta)$ are presented in Table 2.

The wide wavelength range observed allowed us to perform a complete plasma diagnosis. All the available diagnostic line ratios were analyzed. Electron temperatures were derived from the $[O III] \lambda\lambda 4363/5007$ and $[N II] \lambda\lambda 5755/6583$ line ratios and from the $H I$ Balmer discontinuity flux difference relative to $I(H\beta)$. On the other hand, electron densities were derived from the $[S II] \lambda\lambda 6717/6731$, $[S II] \lambda\lambda 4069/6725$ and $[O II] \lambda\lambda 3727/7325$ line ratios. The results are presented in Table 3.

It is found that, for each nebula, the temperatures derived from the forbidden line ratios and $T_e(\text{Bal})$ are equal within the errors. The exception is N 110, where $T_e(\text{Bal})$ is lower than $T_e(\text{FL})$ by more than 2000 K, which is definitely above the uncertainties. Similarly large electron temperature variations, determined from different methods and different ions, have been found for some galactic PNe. They have been interpreted as large

temperature fluctuations inside the nebula (e.g., Peimbert 1971; Liu & Danziger 1993).

Electron densities derived from different line ratios show large variations that could be attributed to uncertainties in the faint line intensities used for diagnosis. This is evident in Ln 302, where there is a huge discrepancy between $N_e(S II \lambda\lambda 6717/6731)$ and the values from other density dependent line ratios. For the abundance calculations, we have adopted average densities, $\langle N_e \rangle$, for all the objects except Ln 302, for which we have used the low density value that seems to be more reliable. Our results are consistent with density determinations made by Barlow (1987), from the $[O II] \lambda\lambda 3726/3729$ intensity ratio. Barlow's values are also listed in Table 2.

Most of the objects have electron densities well above 10^4 cm^{-3} . The only exceptions are LM 1-64, whose nucleus is a “weak emission line star” (see Sect. 5), and Ln 302 which, according to Barlow (1987), seems to be an old PN surrounding a low mass star which evolves slowly. Therefore, in general, MC WR-PNe are denser than the bulk of MC PNe. This is not the case for galactic WR-PNe whose densities are similar to those of non WR-PNe (Gorny & Stasińska 1995). Furthermore, a systematic trend has been reported by Acker et al. (1996) for galactic WR-PNe, in the sense that PNe ionized by late WR stars are denser than those ionized by early WR stars; therefore late WR-PNe would be younger than early WR-PNe. Following these ideas, the MC WR-PNe, except Ln 302, should be very young nebulae.

From the dereddened $H\beta$ fluxes, the physical conditions (electron temperature and density) and the distance, we have calculated the nebular ionized masses. Distance moduli of 18.80 and 18.45 were adopted for the SMC and the LMC respectively (Feast 1991). The results have been included in Table 3. We found that the nebulae in our sample have ionized masses lower than $0.1 M_{\odot}$ (which is another sign of young nebulae). The exception is again Ln 302, for which Barlow (1987) derived an ionized mass of $0.21 M_{\odot}$, consistent with an evolved PN.

4. Ionic and chemical abundances

Ionic abundances for He^+ , He^{++} , N^+ , O^+ , O^{++} , Ne^{++} , Ar^{++} , Ar^{+3} , Ar^{+4} , S^+ , and S^{++} were derived from the optical data. A two-temperature zone scheme was adopted: $T_e(N II)$ was used for the singly-ionized species and S^{++} ; $T_e(O III)$ was employed for all the other ions and He^+ . The average densities were used in all the cases. Abundances of C^{++} were derived from the UV $C III] \lambda 1909$ collisionally excited line and from the $C II \lambda 4267$ recombination line, which seems to be of nebular origin for all the objects. In the latter case we used the expression (3) by Peimbert et al. (1995).

The results are presented in Table 3, where we included the uncertainties for the physical parameters and the ionic abundances. To derive ionic abundance uncertainties we considered the errors due to electron temperature and density uncertainties. For the majority of the ions, the main contribution to uncertainties comes from temperature errors, but for the density sensitive

Table 2. Observed nebular UV and optical fluxes, relative to H β .

$\lambda(\text{\AA})$	ion	Observed Flux						
		N 110 ^a	N 133 ^a	N 203 ^a	LM 1-64 ^a	MA 17 ^{a,c}	N 6 ^b	Ln 302 ^{b,d}
1240	N v	—	18.9:	—	—	—	—	—
1550	C IV	stellar	stellar	stellar	185.2	—	—	—
1640	He II	—	29.2:	—	363	—	—	—
1909	C III]	276	235	241	1288	—	—	—
3346	[Ne v]	—	—	—	27.0	—	—	—
3423	[Ne v]	—	—	—	53.3	—	—	—
3726+29	[O II]	54.0	10.3	72.1	84.4	292	12.0	425
3835	H9	6.4	6.5	6.7	6.7	—	5.8	7.5
3869	[Ne III]	89.0	38.0	37.7	91.1	—	51.8	—
3889	H8 + He I	17.2	12.4	17.0	14.9	9.9	14.0	21.4
3967+70	[Ne III] + H7	42.2	27.4	26.7	41.5	8.4	29.7	13.1
4026	He I + He II	2.3	2.3	2.3	1.9	—	2.1	—
4069	[S II]	4.2	1.7	2.7	6.3	7.8	2.7	3.1
4102	H δ	23.3	24.1	23.5	22.3	19.5	21.3	25.4
4269	C II	1.5	1.2	1.3	1.0	—	0.9:	—
4340	H γ	43.6	45.0	44.3	41.4	49.0	40.9	49.5
4363	[O III]	9.3	7.9	5.4	14.6	9.0	13.0	—
4471	He I	5.0	5.2	4.8	2.8	—	5.1	—
4541	He II	—	—	—	1.7	—	—	—
4686	He II	stellar?	stellar?	stellar?	49.0	—	stellar?	stellar?
4711+13	[Ar IV] + He I	1.3	1.1	0.7	2.7	—	1.4	—
4725	[Ne IV]	—	—	—	0.8:	—	—	—
4740	[Ar IV]	0.9	—	0.2	2.4	—	1.2	—
4861	H β	100	100	100	100	100	100	100
4921	He I	1.4	1.4	1.4	1.0	—	1.5	—
4959	[O III]	410	250	234	387	176	266	35.4
5007	[O III]	1210	sat	sat	sat	476	798	100.
5200	[N I]	0.4:	1.0:	0.3:	0.8:	—	0.7:	—
5411	He II	—	0.6:	0.4:	4.7	—	—	—
5517	[Cl III]	0.2:	—	0.3:	—	—	—	—
5538	[Cl III]	0.6:	—	0.4:	—	—	—	—
5755	[N II]	1.4	0.5:	0.8	1.5	—	2.9	—
5876	He I	19.6	19.0	17.5	12.4	15.6	22.6	—
6300	[O I]	11.8	2.1	4.8	15.0	—	5.3	—
6312	[S III]	1.9	1.6	1.4	2.1	—	2.1	—
6363	[O I]	3.9	0.8	1.5	5.1	—	1.9	—
6548	[N II]	19.0	—	12.0	18.6	66.7	18.0	29.7
6563	H α	355	320	327	344	469	417	257
6583	[N II]	55.7	10.3	36.7	66.5	240	47.0	117
6678	He I + He II	5.4	5.3	4.8	3.5	11.7	5.7	—
6717	[S II]	3.1	0.3:	2.4	5.4	11.7	0.9	5.9
6731	[S II]	6.0	0.7:	4.4	9.6	26.3	1.9	17.5
7006	[Ar v]	—	—	—	1.2	—	—	—
7065	He I	12.0	15.7	9.7	7.0	22.8	18.7	—
7136	[Ar III]	15.9	9.5	10.3	11.5	19.7	12.3	—
7320+30	[O II]	23.0	11.9	17.0	27.4	132	16.0	16.3
$\log F(\text{H}\beta)$ (erg cm ⁻² s ⁻¹)		-12.70	-12.59	-12.61	-12.82	-13.56	-12.77	-13.50
c(H β)		0.25	0.20	0.18	0.30	0.67	0.46	-0.12

^a LMC objects.^b SMC objects.^c Data from Vassiliadis et al. (1992).^d Data from Vassiliadis et al. (1992) and Barlow (1987).

Table 3. Physical conditions^a, ionized masses and ionic abundances, relative to H⁺

	N 110	N 133	N 203	LM 1-64	MA 17	N 6	Ln 302
$T_e(\text{N II}) (10^4 \text{ K})$	1.16±0.10	1.40±0.20	1.08±0.10	1.15±0.10	—	1.70±0.10	—
$T_e(\text{O III}) (10^4 \text{ K})$	1.10±0.07	1.16±0.07	1.06±0.07	1.30±0.05	1.50±0.15	1.45±0.05	—
$T_e(\text{Bal}) (10^4 \text{ K})$	0.80±0.15	1.05±0.15	1.02±0.15	1.40±0.15	—	1.60±0.15	—
$N_e(\text{S II } 6717/6731)$	7.9	22.:	5.8	5.6	≥50	13.7	≥50
$N_e(\text{S II } 4069/6725)$	12.6	32.9	11.0	8.0	≈10	36.7	2.0
$N_e(\text{O II } 3727/7325)$	18.8	52.4	15.0	9.1	≈10	35.0	≈3.0
$\langle N_e \rangle$	13±5	35±10	11±4	7.6±2	10	28±8	1.0
$N_e(\text{O II})^b$	13	66	30	—	—	26	0.93
$M_{ion} (M_\odot)$	0.054	0.022	0.066	0.10	—	0.061	0.21 ^b
$\log \text{He}^+$	-0.88 ± 0.005	-0.90 ± 0.005	-0.92 ± 0.005	-1.07 ± 0.004	-1.04	-0.91 ± 0.004	—
$\log \text{He}^{++}$	—	—	—	-1.36 ± 0.004	—	—	—
$\log \text{N}^+$	-5.20 ± 0.06	-6.00 ± 0.10	-5.25 ± 0.06	-5.11 ± 0.06	-4.96:	-5.56 ± 0.06	-4.88:
$\log \text{C}^{++}(\lambda 1909)$	-3.22 ± 0.12	-3.38 ± 0.12	-3.16 ± 0.12	-3.26 ± 0.10	—	—	—
$\log \text{C}^{++}(\lambda 4267)$	-2.83 ± 0.01	-2.92 ± 0.01	-2.90 ± 0.01	-2.94 ± 0.01	—	-2.96 ± 0.01	—
$\log \text{C}^{+3}$	—	—	—	-3.23 ± 0.10	—	—	—
$\log \text{O}^+$	-4.45 ± 0.12	-5.14 ± 0.20	-4.26 ± 0.12	-4.38 ± 0.10	-3.44:	-5.36 ± 0.12	-4.15:
$\log \text{O}^{++}$	-3.44 ± 0.08	-3.79 ± 0.08	-3.68 ± 0.08	-3.77 ± 0.06	-4.29:	-4.04 ± 0.06	-4.96:
$\log \text{Ne}^{++}$	-4.17 ± 0.10	-4.62 ± 0.08	-4.48 ± 0.10	-4.38 ± 0.05	—	-4.74 ± 0.05	—
$\log \text{Ar}^{++}$	-6.22 ± 0.06	-6.46 ± 0.06	-6.25 ± 0.06	-6.20 ± 0.04	-6.66:	-7.07 ± 0.04	—
$\log \text{Ar}^{+3}$	-6.91 ± 0.10	-7.23 ± 0.10	-7.45 ± 0.08	-6.67 ± 0.06	—	-7.02 ± 0.05	—
$\log \text{Ar}^{+4}$	—	—	—	-7.20 ± 0.05	—	—	—
$\log \text{S}^+$	-6.42 ± 0.14	-7.08 ± 0.20	-6.49 ± 0.14	-6.38 ± 0.10	-5.85:	-7.04 ± 0.15	—
$\log \text{S}^{++}$	-5.76 ± 0.10	-6.11 ± 0.10	-5.75 ± 0.10	-5.66 ± 0.06	—	-6.28 ± 0.06	—

^a Density in units of 10^3 cm^{-3} .^b Data from Barlow (1987).**Table 4.** Chemical composition of the LMC WR-PNe

	N 110	N 133	N 203	LM 1-64	MA 17	$\langle \text{LMC-PN} \rangle^a$	$\langle \text{LMC H II} \rangle^b$
$\log \text{He}/\text{H}^c$	11.12 ± 0.01	11.10 ± 0.01	11.08 ± 0.01	11.11 ± 0.01	10.96 ± 0.10	11.00 ± 0.05	10.93 ± 0.02
$\log \text{O}/\text{H}^c$	8.60 ± 0.10	8.22 ± 0.15	8.42 ± 0.10	8.45 ± 0.08	8.20 ± 0.20	8.42 ± 0.13	8.43 ± 0.08
$\log \text{N}/\text{O}$	-0.75 ± 0.10	-0.86 ± 0.10	-0.99 ± 0.10	-0.73 ± 0.08	-0.95 ± 0.15	-0.76 ± 0.30	-1.46 ± 0.18
$\log \text{C}/\text{O}^d$	0.22 ± 0.12	0.41 ± 0.12	0.52 ± 0.12	0.70 ± 0.12	—	0.38 ± 0.30	-0.50 ± 0.15
$\log \text{C}/\text{O}^e$	0.61 ± 0.10	0.87 ± 0.10	0.78 ± 0.10	0.77 ± 0.10	—	—	—
$\log \text{Ne}/\text{O}$	-0.73 ± 0.12	-0.83 ± 0.12	-0.80 ± 0.12	-0.61 ± 0.12	—	-0.82 ± 0.30	-0.79 ± 0.18
$\log \text{S}/\text{O}$	-2.07 ± 0.20	-1.91 ± 0.20	-1.97 ± 0.20	-1.82 ± 0.20	—	-1.95 ± 0.30	-1.58 ± 0.20
$\log \text{Ar}/\text{O}$	-2.72 ± 0.20	-2.60 ± 0.20	-2.59 ± 0.20	-2.45 ± 0.20	-2.37 ± 0.3	-2.56 ± 0.30	-2.23 ± 0.14

^a Data for non Type I LMC PNe from Barlow (1991) and Clegg (1993).^b Data from Dufour (1984, 1990).^c In units of $12 + \log \text{O}/\text{H}$.^d From the C III] $\lambda 1909$ line.^e From the C II $\lambda 4267$ line.

lines, [O II] $\lambda 3727$ and [S II] $\lambda \lambda 6717+31$, the main uncertainty comes from the density errors.

As it has been previously pointed out by several authors, frequently there is a large discrepancy between the C⁺⁺ abundance derived from the C II $\lambda 4267$ recombination line and that derived from the C III] $\lambda 1909$ collisionally excited line, in the sense that C⁺⁺($\lambda 4267$) \gg C⁺⁺($\lambda 1909$). We found this phenomenon in all our objects with both lines measured. In all cases C⁺⁺($\lambda 4267$) / C⁺⁺($\lambda 1909$) ≥ 2 . Recent discussions of the possible causes for this discrepancy can be found in Rola & Stasińska (1994) and

Peimbert et al. (1995). Following Peimbert et al. we will adopt the C⁺⁺($\lambda 4267$) abundance as representative for all the objects.

Total abundances of He, N, C, O, Ar, and S, relative to H, were obtained from the ionic abundances and the ionization correction factors from the compilation by Kingsburgh & Barlow (1994), to correct for the unseen ionization stages. The expressions used are:

$$\frac{\text{O}}{\text{H}} = \left(\frac{\text{O}^+ + \text{O}^{++}}{\text{H}^+} \right) \times \left(\frac{\text{He}^+ + \text{He}^{++}}{\text{He}^+} \right)^{2/3}, \quad (2)$$

Table 5. Chemical composition of the SMC WR-PNe.

	N 6	Ln 302 ^a	<SMC-PN> ^b	<SMC-H II> ^c
log He/H	11.07 ± 0.01	–	10.99 ± 0.08	10.90 ± 0.02
log O/H	7.98 ± 0.08	7.92	8.24 ± 0.11	8.02 ± 0.08
log N/O	−0.19 ± 0.15	−0.73	−0.73 ± 0.20	−1.56 ± 0.18
log C/O	1.08 ± 0.20	–	0.62 ± 0.27	−0.74 ± 0.15
log Ne/O	−0.70 ± 0.12	–	−0.82 ± 0.20	−0.80 ± 0.20
log S/O	−1.90 ± 0.20	–	−1.80 ± 0.35	−1.53 ± 0.20
log Ar/O	−2.64 ± 0.20	–	−2.63 ± 0.25	−2.24 ± 0.14

^a Data from Monk et al. (1988).

^b Data for non Type I SMC PNe from Barlow (1991) and Clegg (1993).

^c Data from Dufour (1984, 1990).

$$\frac{N}{H} = \frac{N^+}{H^+} \times \frac{O}{O^+}, \quad (3)$$

$$\frac{C}{H} = \frac{C^{++}}{H^+} \times \frac{O}{O^{++}}, \quad (4)$$

$$\frac{Ne}{H} = \frac{Ne^{++}}{H^+} \times \frac{O}{O^{++}}, \quad (5)$$

$$\frac{Ar}{H} = \frac{Ar^{++} + Ar^{+3} + Ar^{+4}}{H^+} \times \left(\frac{1}{1 - N^+/N} \right), \quad (6)$$

$$\frac{S}{H} = \left(\frac{S^+ + S^{++}}{H^+} \right) \times \left(1 - \left(1 - \frac{O^+}{O} \right)^3 \right)^{-1/3}. \quad (7)$$

Temperature fluctuation effects were not included, therefore the chemical abundances obtained from collisionally excited lines should be considered as lower limits to the real abundances. On the other hand, the abundances relative to O are less dependent on the adopted temperature and, therefore, are more reliable. Abundance ratios for the LMC objects are presented in Table 4 where we also list, for comparison, the average abundances for the LMC PNe and H II regions as given by Barlow (1991), Clegg (1993) and Dufour (1984, 1990) respectively. The values for SMC N 6 and Ln 302 are presented in Table 5.

One important conclusion from Table 4 is that all studied WR-PNe in the LMC are extremely C-rich relative to H II regions. If we take the C abundance derived from the C II $\lambda 4267$ line, the C/O ratios are in the range from 4 to 7, which represents enrichments by factors of 13 to 20. Even if we take the C abundances derived from the C III] $\lambda 1909$ emission lines, the enrichments would be by factor of 5 to 16. Similar C enrichments have been found for other samples of LMC PNe (Aller et al. 1987; Walton et al. 1991). According to Walton et al. (1991), non Type I PNe in the LMC have a mean value $\log C/O = -0.38$ which represents a C enhancement by a factor 7.6 relative to H II regions. The large C enrichment can only be explained as due to contamination by freshly made C. It is important to point out that the WC central stars of the PNe in this work have been ejecting He- and C-rich material for more than 20 years (at least since their discovery as WC type stars). According to recent expanding atmosphere models for WC PN nuclei (Hamann 1996;

Leuenghagen et al. 1996; Koesterke & Hamann 1996), the typical mass loss rate in these stars is about $10^{-6} M_{\odot} \text{ yr}^{-1}$ and as much as 50% of the ejecta could be C. This amounts to more than $10^{-5} M_{\odot}$ of freshly made C ejected by the wind, contaminating the inner part of the nebular envelope.

With regard to the nitrogen present in the LMC objects, we found a mean N/O ratio which is a factor of about 7 larger than the mean N/O value of H II regions; although none of them can be classified as a Type I PN (Peimbert 1978). Large N enrichments have been found in every other sample of LMC PNe (see Table 4). These large N abundances in PNe are consistent with an efficient C to N conversion during the CN-cycle. Furthermore, N and C enhancements in PNe have been interpreted as evidence of the dredge-up processes in the central star. As pointed out by Iben & Renzini (1983), the first and second dredge-up episodes extract N enhanced material from the CN- and CNO-cycles (the second one occurs only in stars more massive than $3 M_{\odot}$), while the third one extracts freshly made C to the stellar surface. In the case of Type I PNe (where the nebular N abundance exceeds the original C+N value for H II regions), an additional C to N conversion, due to hot-bottom-burning or envelope burning, has been invoked (Kingsburgh & Barlow 1994). This suggests that the N enrichment observed in our LMC objects is due to CN-cycle only.

Concerning other elements, we found that O, Ne, Ar and S abundances are similar to the values found in H II regions and PNe, indicating that these elements have not been affected by stellar nucleosynthesis.

In conclusion, except for the high densities and large C enrichments, the LMC WR-PNe are like normal non Type I PNe. Likewise, the mean chemical abundances of galactic WR-PNe are similar to those of PNe with non WR nuclei (the C abundance does not seem to be specially enhanced in galactic WR-PNe, as discussed by Gorny & Stasińska 1995).

In the case of the SMC WR-PNe (Table 5), we found that N 6 is a He- and N-rich nebula which can be classified as Type I. The N abundance is larger than the (C + O) abundance found in H II regions, therefore the hot-bottom burning must have occurred in this object. Additionally, the C abundance, as derived from the C II recombination line, is very enhanced, showing an even larger enrichment than the LMC objects. Therefore the central star of SMC N 6 also has undergone the third dredge-up process. In Table 5 we have included the O and N abundances of Ln 302, as derived from ionic abundances. However, these values are very uncertain because large amounts of neutral material could exist in this very low excitation nebula.

5. Characteristics of the central stars

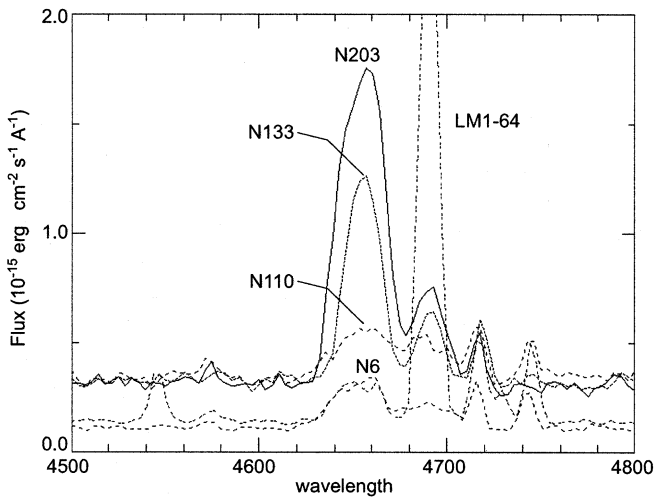
5.1. Spectral classification

Details of the stellar spectral features in the $\lambda\lambda 4650$ and 5808 regions are presented in Figs. 3 and 4. Significant differences are found among the different objects. The central star of N 203 shows the brightest and widest carbon features while that of LM 1-64 shows the faintest and narrowest ones. It is clear that

Table 6. Line fluxes, equivalent widths and fwhm of stellar lines^a

		N 110			N 133			N 203			LM 1-64			N 6		
$\lambda(\text{\AA})$	ion	flux	ew	fwhm	flux	ew	fwhm	flux	ew	fwhm	flux	ew	fwhm	flux	ew	fwhm
1550	C IV	80	38	7	105	36	12	210	60	10	nebular			—	—	—
4442	C IV	0.7	4	16	1.9	7	13	1.6	5	18	—	—	—	1.0:	8	20:
4650	C III	7.8	44	35	21.5	76	21	47.2	170	28	4.4	32	22	7.7	79	33
4686	He II	3.7	21	24	5.1	18	14	9.0	32	17	nebular			2.6	23	24
5592	O V	0.8	4	28	1.4	7	21	0.9:	4:	11:	—	—	—	—	—	—
5696	C III	—	—	—	1.3	7	20	1.0:	5:	14:	—	—	—	—	—	—
5808	C IV	18.5	92	38	13.1	57	22	31.9	128	27	1.7	10	16	15.7	129	31

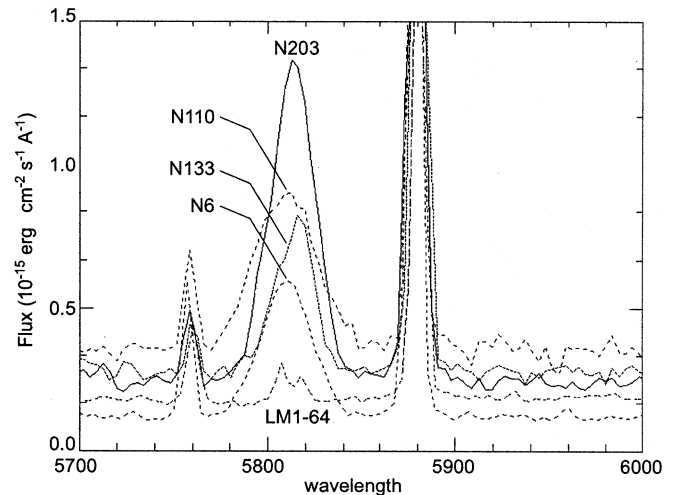
^a Flux in units of 10^{-15} erg cm^{-2} s^{-1} . Equivalent width (ew) and full width at half maximum (fwhm) in \AA .

**Fig. 3.** Details of the stellar spectra around the C III $\lambda 4650$ emission line.

there are faint stellar He II $\lambda 4686$ emission lines in most of the objects, except in LM 1-64 for which this emission is clearly nebular. In Table 6 we present the fluxes, equivalent widths and full widths at half maximum of the stellar lines.

Although most of the stellar features are very faint, we intended to classify the stellar spectra following the qualitative and quantitative criteria given by van der Hucht et al. (1981), Méndez & Niemela (1982) and Torres et al. (1986). We derived WC 4–5 spectral types for N 110 and SMC N 6 and WC 5–6 spectral types for N 133 and N 203. These results are in good agreement with previous classifications (Monk et al. 1988). The faintness of the stellar lines in LM 1-64 does not allow a reliable classification; this star is very similar to the “weak emission-line central stars” described by Tylenda et al. (1993). Tentatively a WC-Of spectral type will be attributed to this star. Concerning the other objects, as indicated in Sect. 1, LMC MA 17 was classified as a WC 7 type star by Hamann (1996) and SMC Ln 302, as a WC 8 star by Monk et al. (1988).

It is worth pointing out that all these objects show WC 4–5 to WC 8 spectral types, while in the Galaxy, WR-PN central stars

**Fig. 4.** Details of the stellar spectra around the C IV $\lambda 5808$ doublet.

are mostly concentrated in the WC 3–4 and WC 8–11 types, with very few objects in the intermediate classes (Tylenda et al. 1993). In this sense, although we are dealing with a few objects, the WR-PNe in the Magellanic Clouds show a spectral type distribution significantly different with respect to that of their counterparts in the Galaxy. Similar differences are found in the Population I WC spectral classes. Conti & Massey (1989) reported that, in a sample of 12 population I WC stars in the LMC, all of them show WC 4 spectral types. No late WC stars were found, in contrast to what is the case in the Galaxy. This interesting phenomenon is probably related to the differences in chemical composition between the Milky Way and the Clouds and it certainly deserves further investigation.

5.2. Stellar parameters

Apparent visual magnitudes were derived for the central stars, from the continuum measurements at $\lambda 5480$ in the $10''$ slit spectra, after subtraction of the nebular continuum. From these data we determined the stellar absolute visual magnitudes and the H I Zanstra temperatures (assuming a black-body behavior). In

Table 7. Stellar parameters.

object	M_V^a	$T_Z(\text{H})$	$T_Z(\text{He II})$	T_{color}^b
N 110	0.8:	70 000:	—	60 000:
N 133	0.8	60 000	—	90 000
N 203	1.4	75 000	—	110 000
LM 1-64	1.3	65 000	100 000	150 000:
SMC N 6	0.5	65 000	—	—

^a The uncertainties are about 0.5 mag, being higher for N 110.

^b The uncertainties are of $\pm 20\,000$.

the case of LM 1-64, we also determined the He II Zanstra temperature. The results are presented in Table 7. The magnitude determinations have uncertainties smaller than 0.5 mag, except for LMC N 110 central star where the uncertainty is larger. This object is located in an extremely crowded region and it is therefore very difficult to extract the stellar continuum without contamination of the neighboring stars.

Color temperatures were also determined for the stars with IUE observations. This was made by using the dereddened UV to optical color index $\lambda\lambda 1550/5480$ and assuming a black-body behavior. The results are presented in column 5 of Table 7. We can see that all the stars show H I Zanstra temperatures over 60 000 K. In LM 1-64, the He II Zanstra temperature resulted to be 30 000 K higher than the H I temperature; which is normal considering that the nebula could be optically thin to H Lyman photons. On the other hand, the color temperatures are also higher than the H I Zanstra temperatures in all the well determined objects, although they agree within the uncertainties. The high temperatures derived for these stars are in very good agreement with the temperature of 100 000 K derived specifically for the central star of LMC MA 17 (a WC 7 type star, Hamann 1996) from an expanding atmosphere model. For the other objects of earlier WC types, higher temperatures should be expected.

It is interesting to notice that such large stellar temperatures do not produce highly ionized nebulae (the lack of nebular He II lines is evident in all the objects except in LM 1-64) due to the He- and C-rich stellar atmospheres that absorb most of the extreme UV ionizing photons ($\lambda \leq 228 \text{ \AA}$). In comparison with a black body atmosphere of the same temperature, these stars emit much fewer hard UV photons (Koesterke & Hamann 1996). For this reason, the photoionization models made for N 203 and N 133 (Dopita & Meatheringham 1991; Zijlstra et al. 1994), employing black body approximations for the ionizing fluxes, required much lower and unrealistic effective temperatures.

6. Conclusions

From UV and optical spectrophotometric data of MC WR-PNe we have derived the physical conditions and chemical composition of the nebulae and some stellar parameters.

The nebular gas is extremely C-rich probably due to contamination with freshly-made C from stellar nucleosynthesis. The other elements show normal behavior when compared with

the bulk of PNe in the Clouds. The only Type I PN in our sample is SMC N6 which is also C-rich. Most of the nebulae have large electron densities ($N_e \geq 10^4 \text{ cm}^{-3}$) which has been interpreted as an indication of youth. The exception is SMC Ln 302 that is a very low excitation and probably old nebula. Except for the high densities and large C enrichment the MC WR-PNe appear as perfectly normal PNe.

All the central stars, except for the progenitor of LM 1-64, show broad carbon features indicating spectral types in the range from WC 4–5 to WC 8. The central star of LM 1-64 is a “weak emission line star”. The WR spectral type distribution of the MC WR-PNe is very different with respect to that found for galactic planetary nebulae with WR nuclei, where most of the objects are concentrated in the WC 3–4 and WC 8–11 types.

Estimates of the H I Zanstra temperatures indicate that the WR-PN central stars studied in this work are hotter than 60 000 K. The temperatures derived from the $\lambda\lambda 1500/5480$ color index are higher than the respective H I Zanstra temperatures. The high temperatures are in good agreement with the spectral types derived for these objects if we consider that the temperature derived from an expanding atmosphere model for LMC MA 17 (a WC 7 star) is 100 000 K.

Acknowledgements. We would like to thank M. Peimbert, L. Koesterke and M. Heydari-Malayeri for fruitful suggestions. M.P. thanks technical support of the staff members at Observatorio de Cerro Calán, Universidad de Chile. This work received partial support from DGAPA/UNAM, CONACyT/México–CONICYT/Chile, FONDECYT-Chile (grant # 1950588) and Cátedra Presidencial (Ciencias) 1996, Chile.

References

- Aller L.H., Keyes C.D., Maran S.P., et al., 1987, *ApJ*, 320, 159
 Barlow M., 1987, *MNRAS*, 227, 161
 Barlow M., 1991, in *The Magellanic Clouds*, IAU Symp. 148, eds. R. Haynes & D. Milne, Kluwer, Dordrecht, p. 291
 Bianchi L., Vassiliadis E., & Dopita M., 1997, preprint
 Clegg R.E.S., 1993, in *Planetary Nebulae*, IAU Symp. 155, ed. R. Weinberger & A. Acker, Kluwer, Dordrecht, p. 549
 Conti P.S., & Massey P., 1989, *ApJ*, 337, 251
 Dopita M.A., & Meatheringham S.J., 1991, *ApJ*, 367, 115
 Dufour R.J., 1984, in *Structure and Evolution of the Magellanic Clouds*, IAU Symp. 108, eds. S. van den Bergh & K.S. de Boer, Reidel, Dordrecht, p. 353
 Dufour R.J., 1990, in *Evolution in Astrophysics: IUE Astronomy in the Era of the New Space Missions*, ESA (SEE N91 -17861), 117
 Feast M.W., 1991, in *The Magellanic Clouds*, IAU Symp. 148, eds. R. Haynes & D. Milne, Kluwer, Dordrecht, p. 1
 Gorny S.K., & Stasińska G., 1995, *A&A*, 303, 893
 Hamann W.-R., 1996, in *Hydrogen Deficient Stars*, ASP Conference Series 96, eds. C.S. Jeffery & U. Heber, Bookcrafters Inc., 127
 Hamuy M., Walker A.R., Suntzeff N.B., et al., 1992, *PASP*, 104, 533
 Hummer D.G., & Storey P.J., 1987, *MNRAS*, 224, 801
 Iben I., & Renzini A., 1983, *ARA&A*, 21, 271
 Kingsburgh R.L., & Barlow M.J., 1994, *MNRAS*, 271, 257
 Koesterke L., & Hamann W.-R., 1996, in *Planetary Nebulae*, IAU Symp. 180, eds. H. Habing & H. Lamers, Reidel, Kluwer, in press
 Leuenghagen U., Hamann W.-R., & Jeffery S., 1996, *A&A*, 312, 167
 Liu X.-W., & Danziger J., 1993, *MNRAS*, 263, 256

- Meatheringham S.J., & Dopita M.A., 1991a, *ApJS*, 75, 407
- Meatheringham S.J., & Dopita M.A., 1991b, *ApJS*, 76, 1085
- Méndez R.H., & Niemela V., 1982, in *Wolf-Rayet Stars: Observations, Physics and Evolution*, IAU Symp. 99, eds. C.W.H. de Loore & A. Willis, Reidel, Dordrecht, p. 457
- Monk D.J., Barlow M.J., & Clegg R.E.S., 1988, *MNRAS*, 234, 583
- Morgan D.H., 1994, *A&ASS*, 103, 235
- Nandy K., Morgan D.H., Willis A.J., Wilson R., & Gondhalekar P.M., 1981, *MNRAS*, 196, 955
- Peimbert M., 1971, *Bol. Obs. Tonantzintla y Tacubaya*, 6, 29
- Peimbert M., 1978, in *Planetary Nebulae*, IAU Symp. 76, ed. Y. Terzian, Reidel, Dordrecht, p. 215
- Peimbert M., Torres-Peimbert S., & Luridiana V., 1995, *RevMexAA*, 31, 131
- Peña M., 1995, *RevMexAASC*, 3, 215
- Peña M., Olguín L., Ruiz M.T., & Torres-Peimbert S., 1994a, *RevMexAA*, 28, 27
- Peña M., Peimbert M., Torres-Peimbert S., Ruiz M.T., & Maza J., 1995, *ApJ*, 441, 343
- Peña M., Torres-Peimbert S., Peimbert M., Ruiz M.T., & Maza J., 1994b, *ApJ*, 428, L9
- Peña M., Hamann W.-R., Koesterke, L., et al., 1996, in *Planetary Nebulae*, IAU Symp. 180, eds. H. Habing & H. Lamers, Reidel, Kluwer, in press
- Rola C., & Stasińska G., 1994, *A&A*, 282, 199
- Sanduleak N., & Phillips A.G., 1976, *PASP*, 89, 792
- Torres A.V., Conti P.S., & Massey P., 1986, *ApJ*, 300, 379
- Tylenda R., Acker A., & Stenholm B., 1993, *A&AS*, 102, 595
- van der Hucht K.A., Conti P.S., Lundström I., & Stenholm B., 1981, *Space Sci. Rev.*, 28, 227
- Walton N.A., Barlow M.J., Monk D.J., & Clegg R.E.S., 1991, in *The Magellanic Clouds*, IAU Symp. 148, eds. R. Haynes & D. Milne, Kluwer, Dordrecht, p. 334
- Vassiliadis E., Dopita M.A., Morgan D.H., & Bell J.F., 1992, *ApJS*, 83, 87
- Whitford A.E., 1958, *AJ*, 63, 201
- Zijlstra A.A., van Hoof P.A.M., Chapman J.M., & Loup C., 1994, *A&A*, 290, 228